Infrared Physics & Technology 115 (2021) 103699

Contents lists available at ScienceDirect

Infrared Physics and Technology

journal homepage: www.elsevier.com/locate/infrared

Regular article

Terahertz dual-comb spectroscopy: A comparison between time- and frequency-domain operation modes

Hui Fu [a], Xingle Jiang [a], Jingrui Wu [a], Liang Qiu [a], Yinghao Yuan [a], Xuguang Guo [a,*], Yiming Zhu [a,b,*]

[a] *Shanghai Key Lab of Modern Optical Systems, Terahertz Technology Innovation Research Institute, and Engineering Research Center of Optical Instrument and System, Ministry of Education, University of Shanghai for Science and Technology, 516 Jungong Road, Shanghai 200093, China*
[b] *Shanghai Institute of Intelligent Science and Technology, Tongji University, Shanghai 200092, China*

ARTICLE INFO

Keywords:
Time-domain spectroscopy
Dual-comb spectroscopy
Terahertz frequency comb
Radio frequency comb

ABSTRACT

In terahertz dual-comb spectroscopies (THz-DCSs), electrical time delay lines are utilized to replace the mechanical ones widely used in traditional terahertz time-domain spectroscopic systems (THz-TDSs). Due to the usage of electrical delay line, the sampling time is effectively prolonged and the consecutive terahertz pulses can be sampled continuously, which leads to the improvement of frequency resolution and makes it possible for THz-DCSs work in dual (frequency- and time-domain, FD and TD) operation modes. Here, a THz-DCS is established by using two repetition-frequency-locked femtosecond (fs) lasers with a slight repetition frequency difference. A spectrum analyzer is used to directly record the terahertz spectral data. Alternatively, the terahertz transient pulses are sampled and recorded, and the terahertz spectra are obtained by Fourier transforming the TD data. The experimental results show that the terahertz spectra acquired in FD and TD are in good agreement with each other. For the dual-mode THz-DCS, the wideband terahertz spectral information and the specified narrowband spectral information with high frequency resolution can be simultaneously acquired, which is helpful for searching sharp-peaked fingerprint spectral features in a broad terahertz frequency range.

1. Introduction

Terahertz radiations are electromagnetic waves located between the frequency range of 0.1 THz and 10 THz. Many applications related to terahertz radiations have been developed rapidly in the past two decades. Especially, THz-TDS has been widely used in the characterization of materials [1,2]. Combined with the continuous improvement of nano-micro photonic technology, THz-TDS is expected to be an emerging non-destructive, label-free and sensitive detection method in biomedical field [3]. For example, it can be used to detect blood lipids and lipoproteins [4,5]. In addition, because of high time resolution, THz-TDS has its unique advantages in quantitative exploring the ultrafast dynamical behavior of protein [6]. The energies corresponding to the rotational and vibrational levels of molecules and the low-energy excitations in solid-state matters are in the terahertz band [7–9], which makes THz-TDS be particularly suitable for fingerprint identification and structural characterization of materials [10].

In a traditional THz-TDS, the laser beam from a fs laser is divided into the pump beam and the probe one by a beam splitter. A mechanical time delay line [11] is used to sample the TD signals, and the broadband terahertz spectrum is obtained by Fourier transforming the TD pulse data. In THz-TDS, because the pump and probe beams originate from the same fs pulse, a complete coherence exists between the two beams, and no additional stabilization of the fs laser is needed [12]. However, due to the mechanical sweeping of the optical path difference between the pump beam and the probe one, the frequency resolution (in principle, inverse proportion to the optical path difference) and the measurement speed are severely limited [13]. It is difficult to quickly obtain terahertz spectra with high frequency resolution and accuracy. At the same time, the consecutive terahertz multi-pulses cannot be continuously sampled in traditional THz-TDSs [14,15].

With the developments of carrier phase and repetition frequency stabilization techniques and the synchronization of two fs lasers, the dual-comb sampling (or asynchronous optical sampling) technique [16] was realized. In a dual-comb related measurement system, the pump and probe laser beams are from two synchronized optical frequency combs

* Corresponding authors.
E-mail addresses: xgguo_sh@qq.com, xgguo@usst.edu.cn (X. Guo), ymzhu@usst.edu.cn (Y. Zhu).

https://doi.org/10.1016/j.infrared.2021.103699
Received 6 January 2021; Received in revised form 24 February 2021; Accepted 24 February 2021
Available online 1 March 2021
1350-4495/

[17]. Since there is a small offset frequency $\Delta f = f_2$-f_1 with f_1 and f_2 the repetition frequencies of the master and slave optical frequency combs [18], respectively, there is an increasing time delay between the consecutive pump and probe fs pulses, and the maximum time delay is the repetition period of the pump optical frequency comb. Therefore, the TD signals related to the pump fs laser pulse can be sampled by the probe fs pulse [19]. The dual-comb-based sampling can be considered as an electrical time delay line. In comparison with the traditional sampling based on mechanical time delay line, the dual-comb-based sampling technique has advantages of fast sampling, long sampling time window, continuous sampling of consecutive multi-signal events, and no movable components [20,21].

In 2006, the dual-comb sampling technique was applied to the terahertz spectroscopic systems. In a THz-DCS, a biased photoconductive antenna (PCA) is pumped by the master repetition-frequency-stabilized fs laser, which is a harmonic terahertz comb emitter; another unbiased PCA is pumped by the slave repetition-frequency-stabilized fs laser, in which the terahertz signals are acquired through multi-frequency heterodyne detection [22–24]. In order to increase the frequency resolution and the signal to noise ratio, various relevant techniques have been developed for THz-DCSs [25–27]. By combining of the spectral comb-tooth interleaving technique and the extension of sampling time window up to multiple terahertz pulses, comb-tooth-resolved terahertz spectra with a frequency resolution of 2.5 MHz have been reported [27]. Adaptive sampling and post signal processing algorithms were adopted to recover the coherence of signal and to achieve a long integration (averaging) time [26].

Due to the ability of continuous sampling of multi TD pulses for THz-DCSs, comb-tooth-resolved frequency resolution can be reached. It has been reported that up to 100 consecutive TD pulses were sampled and about 2.5 MHz frequency resolution was obtained [27]. However, to get a broadband terahertz spectrum with such a high frequency resolution, large numbers of data must be recorded, stored, and Fourier transformed. At the same time, it is also a time-demanding task because many times of average are needed to get a high signal-to-noise ratio. In fact, for many applications, it is unnecessary to keep a constant high frequency resolution within the whole broadband spectral range [28]. High frequency resolution is important to observe the fine structure of narrow-peaked fingerprint spectral features. Therefore, it is valuable to develop the spectroscopic technique that a broadband frequency range can be covered with a medium frequency resolution, and the specified narrowband spectra of narrow-peaked features with high frequency resolution can be simultaneously acquired [29].

In this work, two synchronized fs lasers with their repetition frequencies being locked are used to build a THz-DCS. The THz-DCS can be operated simultaneously in FD and TD modes. In the FD mode, the specified narrowband spectral information with high frequency resolution is directly obtained. Alternatively, in TD mode, the TD data are recorded and the terahertz spectra are obtained by Fourier transforming the recorded data. The experimental results show that the FD and TD spectra are in good agreement with each other. For the dual-mode THz-DCS, the broadband terahertz spectrum with medium frequency resolution and the specified narrowband spectrum with high frequency resolution can be simultaneously obtained, which is very helpful for searching sharp-peaked fingerprint spectral features in a broad terahertz frequency range. In this way, a better trade-off among measurement time, data size, frequency resolution, and bandwidth is achieved.

2. Principles of TD and FD THz-DCS

Fig. 1(a) shows the principle of dual-comb spectroscopy in TD. The repetition frequency of the terahertz pulse is f_r, and the repetition frequency of the detection pulse is $f_r + \Delta f$. If we assume at $t = 0$ with t the laboratory time, the detection fs pulse and the start point of terahertz pulse arrive at the PCA detector simultaneously, there is a time delay between the subsequent detection and terahertz pulses at $t = 1/f_r$.

$$\Delta\tau = \frac{1}{f_r} - \frac{1}{f_r + \Delta f} = \frac{\Delta f}{(f_r + \Delta f)f_r} \approx \frac{\Delta f}{f_r^2} \quad (1)$$

At $t = 1/\Delta f$, the terahertz pulse is sampled completely and the total sampling time is $\tau = 1/f_r$. The relationship between the laboratory time t and the sampling time τ can be expressed as $t = \tau \times f_r/\Delta f$. Once the terahertz pulse is sampled completely, the terahertz spectrum can be obtained by Fourier transforming the TD data. As shown in Fig. 1(b), the principle of THz-DCS can also be considered in FD. A terahertz electromagnetic comb is excited by the pump fs laser (the master laser with repetition frequency of f_r) in the biased PCA emitter. On the other hand, a terahertz photocurrent comb is produced by the probe fs laser (the slave laser with repetition frequency of $f_r + \Delta f$) in the unbiased PCA detector. Due to the multi-frequency heterodyne process in the PCA detector, a radio frequency (RF) comb is produced, which can be recorded by a traditional spectrum analyzer. Because there is a constant magnification factor $f_r/\Delta f$, the terahertz spectrum can be directly derived from the measured RF comb spectrum. In this way, the frequency down-converted terahertz FD signal can be recorded and manipulated with traditional electrical instruments. The direct data acquisition in FD also makes the analysis and research of terahertz signals more convenient and comprehensive [30].

Fig. 2(a) shows the schematic diagram of the experimental THz-DCS operating in dual (TD and FD) mode [31]. A commercial control system (Menlo, SYNCRO Locking Electronics) is used to stabilize the repetition frequencies of the master fs laser (Menlo, C-Fiber 780, $f_{r,pump}$ = 100 MHz) and the slave fs laser (Menlo, C-Fiber 780 High Power,

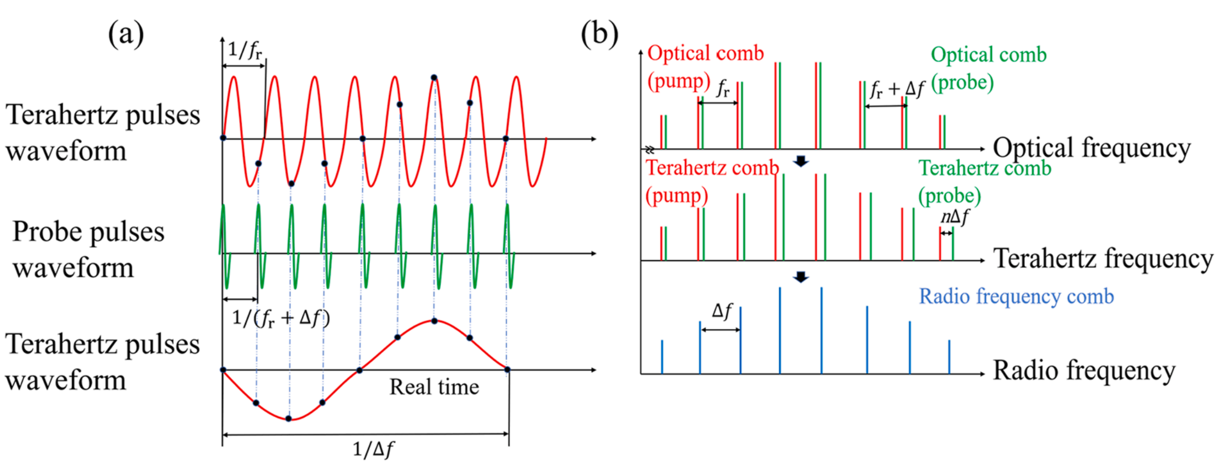

Fig. 1. Principles of THz-DCS in TD (a) and FD (b) modes.

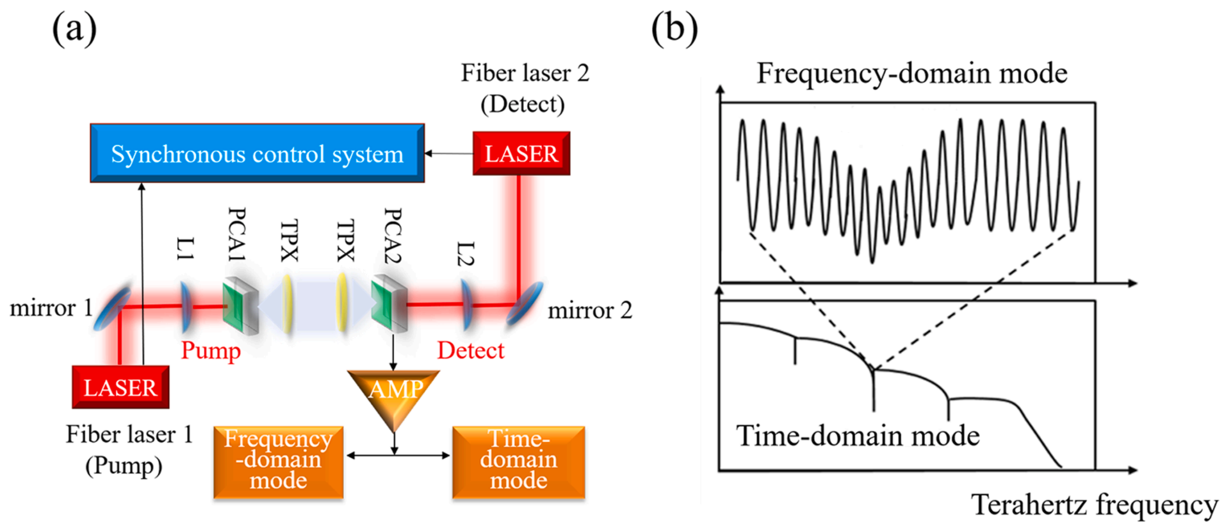

Fig. 2. (a) Schematic diagram of the THz-DCS working in dual mode, and (b) spectra acquired in TD and FD modes.

$f_{r,probe}$ = 100 MHz + 25 Hz). The principle and technique details of the control system can be found in the production manual [32]. A bias voltage of 20 V (KEITHLEY, 2400 source meter) is applied to a low-temperature gallium arsenide (LT-GaAs) strip PCA terahertz emitter (Teravil, ETM-8), which is pumped by the master fs laser. The average power of pump fs pulse is 12 mW, and the photocurrent through the PCA emitter is 0.6 mA. The terahertz pulses are collimated and focused on an unbiased LT-GaAs butterfly PCA terahertz detector (Batop, PCA-44–06-10–800-h) that is gated by the slave fs laser with an average power of 14 mW. The electrical signal from the PCA detector is amplified by a current amplifier (Femto DHPCA-100) with a bandwidth of 1 MHz and a gain of 10^6 V/A. An oscilloscope (Tektronix, MSO 2024B, sampling rate: 1 GSamples/s) is used to collect the terahertz TD signals, and a spectrum analyzer (KEYSIGHT, N9322C, frequency range: 7 kHz-9 GHz, minimum resolution bandwidth: 10 Hz) is used to acquire the FD signals.

As shown in Fig. 2(b), in the TD mode, the terahertz TD pulse is acquired and Fourier transformed to obtain the wideband terahertz spectrum (The terahertz TD pulse is not shown). If we are interested in the detailed information of very sharp spectral features, a very long sampling time window is necessary, which will lead to a huge data set being acquired, stored and manipulated. However, due to the continually electrical optical delay scheme in THz-DCS, the specified narrow-band spectral region where a sharp spectral feature is located, can be directly obtained by using a RF spectrum analyzer, in which a super-heterodyne receiving scheme is adopted. As shown in Fig. 2(b), in the FD mode, a very high frequency resolution can be reached in the narrow

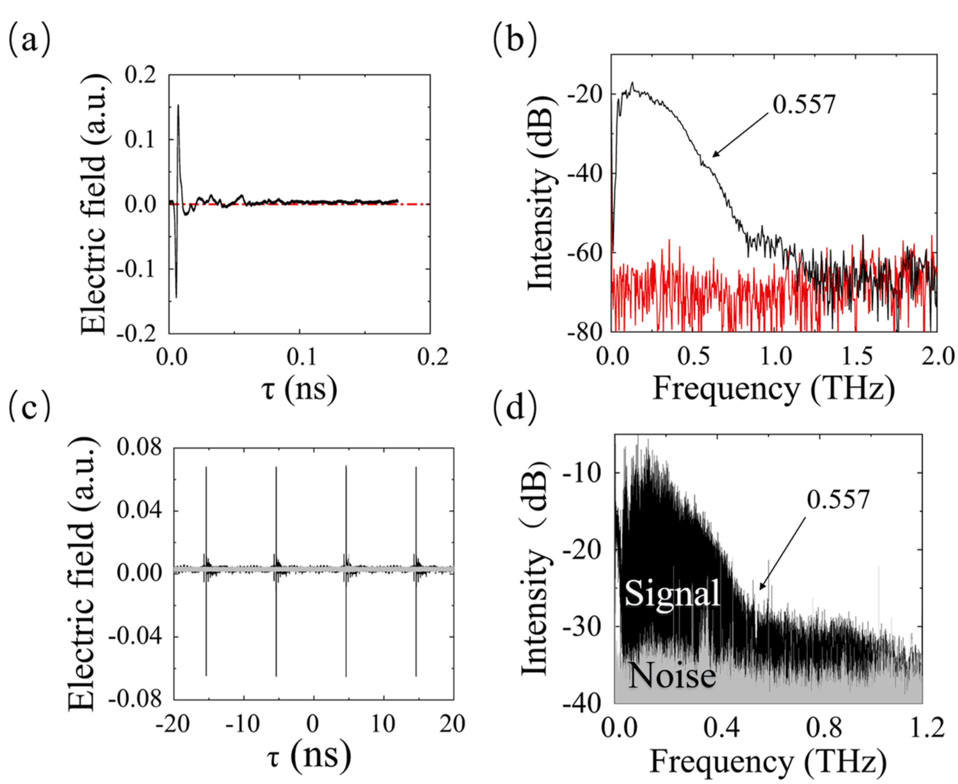

Fig. 3. (a) Terahertz pulse in TD, (b) terahertz spectrum and the noise floor measured in TD mode, (c) TD signal and noise with a sampling time window of 40 ns (four consecutive pulses), (d) and the corresponding comb-tooth-resolved terahertz spectrum and the noise spectrum.

spectral band. Further, as can be seen from Fig. 2, the THz-DCS can be operated in dual mode simultaneously. In this way, the global and local spectral information of the terahertz signal can be studied and analyzed simultaneously. We can freely position the specified narrowband spectral range in the entire spectrum measured in TD. The two signal acquisition methods for parallel measurements are of great significance for studying the terahertz broadband spectrum and narrowband sharp features with high frequency resolution.

3. Results and discussion

All the measurements below are performed at a relative atmospheric humidity of 50% and a room temperature of 298 K. As shown in Fig. 3, to verify the THz-DCS, a terahertz spectrum is firstly measured in TD mode. The oscilloscope is used to collect the TD data, and in order to improve the signal-to-noise ratio, an average of 64 times is performed. The laboratory time t is converted to the real delay time τ by using the relation $\tau = t \times \Delta f / f_r$ to obtain the terahertz TD waveform. The 200-ps-long TD data (Fig. 3(a)) are used to derive the terahertz spectrum. As shown in Fig. 3(b), the terahertz spectrum has a bandwidth of 1.1 THz and a peak energy signal-to-noise ratio of 40 dB. A typical water absorption peak at 0.557 THz is labeled in the spectrum, which is consistent with the reported data in literature [33].

Due to the ability of continually delay-time sampling for THz-DCS, the sampling time window can be extended ($> 1/f_r$), and then a comb-tooth-resolved terahertz spectrum is obtained. As shown in Fig. 3(c), four consecutive terahertz TD pulses and the noise data are acquired and the total sampling time is 40 ns. The Fourier transformed terahertz spectrum and the noise spectrum are shown in Fig. 3(d). Because of the extended delay-time window to 40 ns, the nominal frequency resolution is increased up to 25 MHz without considering the noise influence. Because the frequency resolution is smaller than the repetition frequency f_r, the terahertz comb teeth can be resolved. With the increase of frequency resolution, the spectral intensity and the signal-to-noise ratio decrease, and the maximum terahertz frequency is about 1.0 THz. The water vapor absorption peak at 0.557 THz can be resolved.

Fig. 4 shows the terahertz spectrum acquired in FD mode by using the spectrum analyzer to measure the multi-frequency heterodyne RF signal directly. In order to maintain a high frequency resolution, the resolution bandwidth and the video bandwidth are set to 10 Hz and 1 kHz, respectively.

We collected 160 sets of RF signals from 5 kHz to 165 kHz, and plotted them together to obtain the entire spectrum. After multiplying by the magnification factor $f_r/\Delta f$, the corresponding terahertz spectrum from 0.02 THz to 0.6 THz is obtained. The insert in Fig. 4 shows the narrow band spectrum around 0.06 THz. Due to the high similarity of the RF spectrum and the derived terahertz spectrum, the original RF spectrum is not depicted. The comb teeth are well resolved and the comb tooth spacing is 100 MHz. The profile of the absorption peak is clearly presented (Red line). The noise spectrum in gray color is also shown in Fig. 4. There are two electrical noise peaks located at about 0.35 THz and 0.52 THz, which originate from the environmental electromagnetic interference. In comparison with the terahertz spectrum acquired in TD (Fig. 3), the bandwidth reduction of the spectrum shown in Fig. 4 is due to the data acquisition scheme and the instrumental sensitivity.

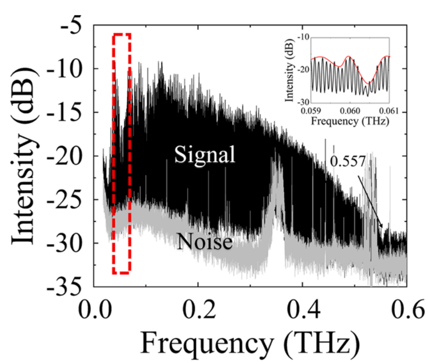

Fig. 4. Terahertz spectra measured in FD by using a RF spectrum analyzer. The noise spectrum shows that there are two strong noise peaks located at about 0.35 THz and 0.52 THz, which originate from the environmental electromagnetic interference.

In order to clearly compare the differences between the two spectra acquired in TD and FD modes, the two spectra are depicted in Fig. 5(a). The relative intensity of the spectrum acquired in TD is multiplied by a constant factor and then the two spectra can be drawn in a smaller intensity scale, which has no influence on the comparison of frequency resolution and frequency accuracy. The intensity of the FD-acquired spectrum decreases faster than that of the TD-acquired one, which originates from the different instrumental transfer functions determined by the different data acquisition methods. It can be seen that the two labeled spectral features at about 0.061 THz and 0.557 THz are consistent well with each other. The zoomed-in narrowband spectra in the frequency range of 0.058–0.062 THz in Fig. 5(b) show that not only the dominant spectral feature, but also the other weak ones are in good agreement with each other, which indicates that the spectral features are not from random fluctuations but from atmospheric absorption or interference between different pairs of optical elements in the THz-DCS. The further zoomed-in narrowband spectra in the frequency range of 0.06–0.0608 THz are shown in Fig. 5(c). Except for the consistent profiles of the spectral feature, the frequencies of comb teeth are also in good accordance with each other, which indicates the excellent frequency stability and accuracy of the THz-DCS and the reliable dual-mode operation. The intrinsic width of terahertz comb tooth is determined by the relative frequency stability of the stabilized repetition frequency of the dual fs lasers, which is dependent on the reference RF source, the bandwidth of phase-lock loop, and the precision of PID controller and actuators. The measured line width of comb tooth is limited by the RBW of spectrum analyzer (10 Hz) in FD and the sampled time window (40 ns) in TD. Thus, the theoretical frequency resolution is 40 MHz in FD and 25 MHz in TD, respectively, both of which are estimated to be larger than the intrinsic width of terahertz comb tooth.

4. Conclusion

A THz-DCS operating in TD and FD modes simultaneously is realized. Because the mechanical time-delay line widely applied in traditional

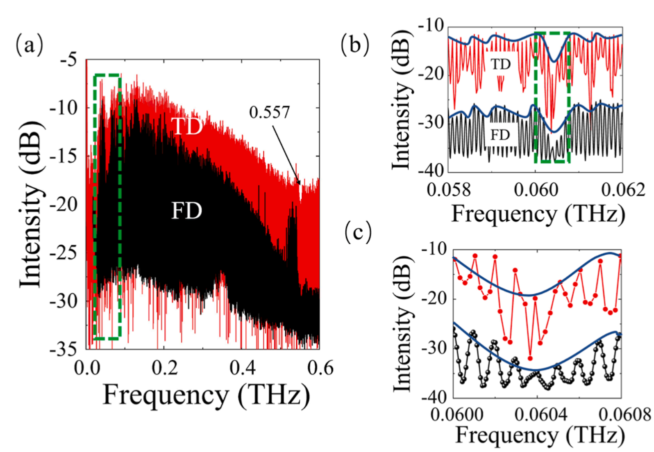

Fig. 5. Comparison of terahertz spectra acquired in TD and FD modes in the frequency range of 0.0–0.6 THz (a), the zoomed-in narrowband spectra in the frequency range of 0.058–0.062 THz (b) and 0.06–0.0608 THz (c). For clarity, the narrow-band spectra acquired in FD shown in Fig. 5(b) and 5(c) are down shifted by 10 dB.

THz-TDS is replaced by the electrical time-delay line in THz-DCS, the sampling time window is easily extended from 100-ps scale to 10-ns scale, which leads to the evident improvement of frequency resolution. At the same time, due to the ability of continuous sampling of multi pulses, the frequency resolution can be further increased and the THz-DCSs can be operated in dual mode (TD and FD). Therefore, the broadband terahertz spectra with moderate frequency resolution (in TD) and the selected narrowband spectra with high frequency resolution can be simultaneously obtained, which is important in real applications. Our experimental results show that the spectra simultaneously acquired in TD and in FD are in good accordance with each other, which indicates the high stability, high frequency resolution, and high frequency accuracy of the dual-mode THz-DCS.

Declaration of Competing Interest

The authors declare that they have no known competing financial interests or personal relationships that could have appeared to influence the work reported in this paper.

Acknowledgements

This work was supported in part by the National Natural Science Foundation of China (61731020, 61988102, and 61722111), the 111 Project (D18014), the Key project supported by Science and Technology Commission Shanghai Municipality (YDZX20193100004960).

References

[1] L. Wang, S. Guilavogui, H. Yin, et al., Critical Factors for In Vivo Measurements of Human Skin by Terahertz Attenuated Total Reflection Spectroscopy, Sensors. 20 (15) (2020) 4256–4270.
[2] M. Tonouchi, Cutting-edge terahertz technology, Nature photonics. 1 (2) (2007) 97–105.
[3] C. Jördens, T. Schlauch, M. Li, et al., All-semiconductor laser driven terahertz time-domain spectrometer, Applied Physics B. 93 (2–3) (2008) 515–520.
[4] Y. Peng, C. Shi, Y. Zhu, et al., Terahertz spectroscopy in biomedical field: a review on signal-to-noise ratio improvement, PhotoniX. 1 (2020) 1–18.
[5] Y. Zhu, Y. Peng, S. Zhuang, Terahertz Imaging and Spectroscopy in Cancer Diagnostics: A Technical Review, A Science Partner Journal. 2020 (2020) 11.
[6] T. Ji, Z. Zhang, H. Zhao, et al., A THz-TDS measurement method for multiple samples, Optics Communications. 312 (2014) 292–295.
[7] S.K. Mathanker, P.R. Weckler, N. Wang, Terahertz (THz) applications in food and agriculture: A review, Transactions of the ASABE. 56 (3) (2013) 1213–1226.
[8] J. Neu, C.A. Schmuttenmaer, Tutorial: An introduction to terahertz time domain spectroscopy (THz-TDS), Journal of Applied Physics. 124 (23) (2018), 231101.
[9] C.B. Reid, G. Reese, A.P. Gibson, et al., Terahertz time-domain spectroscopy of human blood, IEEE journal of biomedical and health informatics. 17 (4) (2013) 774–778.
[10] L. Chen, D. Liao, X. Guo, et al., Terahertz time-domain spectroscopy and micro-cavity components for probing samples: a review, Frontiers of Information Technology & Electronic Engineering. 20 (5) (2019) 591–607.
[11] Y.C. Kim, K.H. Jin, J.C. Ye, et al., Wavelet power spectrum estimation for high-resolution terahertz time-domain spectroscopy, Journal of the Optical Society of Korea. 15 (1) (2011) 103–108.
[12] F. Keilmann, C. Gohle, R. Holzwarth, Time-domain mid-infrared frequency-comb spectrometer, Optics letters. 29 (13) (2004) 1542–1544.
[13] N. Kida, Y. Takahashi, J.S. Lee, et al., Terahertz time-domain spectroscopy of electromagnons in multiferroic perovskite manganites, JOSA B. 26 (9) (2009) A35–A51.
[14] D.M. Mittleman, R.H. Jacobsen, R. Neelamani, et al., Gas sensing using terahertz time-domain spectroscopy, Applied Physics B. 67 (3) (1998) 379–390.
[15] H. Ge, Y. Jiang, F. Lian, et al., Characterization of wheat varieties using terahertz time-domain spectroscopy, Sensors. 15 (6) (2015) 12560–12572.
[16] T. Yasui, E. Saneyoshi, T. Araki, Asynchronous optical sampling terahertz time-domain spectroscopy for ultrahigh spectral resolution and rapid data acquisition, Applied Physics Letters. 87 (6) (2005), 061101.
[17] P.A. Elzinga, R.J. Kneisler, F.E. Lytle, et al., Pump/probe method for fast analysis of visible spectral signatures utilizing asynchronous optical sampling, Applied optics. 26 (19) (1987) 4303–4309.
[18] A. Bartels, A. Thoma, C. Janke, et al., High-resolution THz spectrometer with kHz scan rates, Optics Express. 14 (1) (2006) 430–437.
[19] A. Bartels, R. Cerna, C. Kistner, et al., Ultrafast time-domain spectroscopy based on high-speed asynchronous optical sampling, Review of Scientific Instruments. 78 (3) (2007), 035107.
[20] N. Krauß, A. Nast, D.C. Heinecke, et al., Fiber-coupled high-speed asynchronous optical sampling with sub-50 fs time resolution, Optics express. 23 (3) (2015) 2145–2156.
[21] A. Schliesser, M. rehm, F. Keilmann, et al., Frequency-comb infrared spectrometer for rapid, remote chemical sensing, Optics Express. 13 (22) (2005) 9029–9038.
[22] S. Yokoyama, R. Nakamura, M. Nose, et al., Terahertz spectrum analyzer based on a terahertz frequency comb, Optics express. 16 (17) (2008) 13052–13061.
[23] T. Yasui, Y. Kabetani, E. Saneyoshi, et al., Terahertz frequency comb by multifrequency-heterodyning photoconductive detection for high-accuracy, high-resolution terahertz spectroscopy, Applied Physics Letters. 88 (24) (2006), 241104.
[24] I.A. Finneran, J.T. Good, D.B. Holland, et al., Decade-spanning high-precision terahertz frequency comb, Physical review letters. 114 (16) (2015), 163902.
[25] Y.D. Hsieh, Y. Iyonaga, Y. Sakaguchi, et al., Spectrally interleaved, comb-mode-resolved spectroscopy using swept dual terahertz combs, Scientific reports. 4 (2014) 3816.
[26] T. Yasui, R. Ichikawa, Y.D. Hsieh, et al., Adaptive sampling dual terahertz comb spectroscopy using dual free-running femtosecond lasers, Scientific reports. 5 (1) (2015) 1–10.
[27] H. Li, Z. Li, W. Wan, et al., Toward compact and real-time terahertz dual-comb spectroscopy employing a self-detection scheme, ACS Photonics. 7 (1) (2019) 49–56.
[28] T. Yasui, Y. Iyonaga, Y.D. Hsieh, et al., Super-resolution discrete Fourier transform spectroscopy beyond time-window size limitation using precisely periodic pulsed radiation, Optica. 2 (5) (2015) 460–467.
[29] K. Nitta, C. Jie, T. Mizuguchi, et al., Dual-comb spectroscopy in THz region using a single free-running dual-wavelength mode-locked fiber laser, Proceedings of the SPIE. 10826 (2018) 108260U.
[30] X. Guo, T. Shu, G. You, et al., Photoconductive antenna as local oscillator in terahertz frequency measurement: heterodyne efficiency and bias effect, Optical and Quantum Electronics. 50 (8) (2018) 327.
[31] X.G. Guo, X.L. Jiang, Y.M. Zhu, et al., Unified description on principles of fourier transform infrared spectroscopy and terahertz time-domain spectroscopy, Infrared Physics & Technology. 101 (2019) 105–109.
[32] MenloSystems GmbH SYNCRO Locking Electronics System. https://www.menlosystems.com/, 2021 (accessed 23 February 2021).
[33] H. Cui, X.B. Zhang, J.F. Su, et al., Vibration–rotation absorption spectrum of water vapor molecular in frequency selector at 0.5–2.5 THz range, Optik. 126 (23) (2015) 3533–3537.